The Cryosphere Discuss., 8, 2611–2635, 2014
www.the-cryosphere-discuss.net/8/2611/2014/
doi:10.5194/tcd-8-2611-2014

The Cryosphere Discussions
Open Access

Winter speed-up of quiescent surge-type glaciers in Yukon, Canada

T. Abe and M. Furuya

Department of Natural History Sciences, Graduate School of Science, Hokkaido University, Sapporo, Japan

Received: 4 April 2014 – Accepted: 8 May 2014 – Published: 21 May 2014

Correspondence to: T. Abe (abetaka@frontier.hokudai.ac.jp)

Published by Copernicus Publications on behalf of the European Geosciences Union.

Winter speed-up of quiescent surge-type glaciers in Yukon, Canada

T. Abe and M. Furuya

Abstract

Glacier surge is known to often initiate in winter, but the mechanisms remain unclear in light of the summer speed-up at normal glaciers. We examined spatial-temporal changes in the ice velocity of surge-type glaciers near the border of Alaska and Yukon, and found significant upstream accelerations from fall to winter, regardless of surging episodes. Moreover, whereas the summer speed-up was observed downstream, the winter speed-up propagated from upstream to downglacier. Given the absence of upstream surface meltwater input in winter, we speculate the presence of water storages near the base that do not directly connect to the surface but can promote basal sliding through increased water pressure as winter approaches. Our findings have implications for modeling of glacial hydrology in winter time, and its link to glacier dynamics and subglacial erosion.

1 Introduction

Ice flow at mountain glaciers and ice sheet typically exhibits the greatest acceleration from spring to early summer, followed by deceleration in mid-summer to fall, and is slowest in winter (e.g., Iken and Bindschadler, 1986; Zwally et al., 2002; Sundal et al., 2011; MacGregor et al., 2005; Bartholomaus et al., 2008). These velocity changes are attributed to subglacial slip associated with water pressure changes that occur because of the seasonal variability of meltwater input (Schoof, 2010). The subglacial slip velocity also controls the efficiency of glacial erosion (Iverson, 1991; Hallet, 1996), which produces basal till and, over the geological long term, can limit the height of mountain ranges (e.g., Berger et al., 2008; Egholm et al., 2009; Thomson et al., 2010). A simple rule that relates the rate of glacial erosion to the subglacial slip velocity has been widely used in numerical models of landscape evolution (Thomson et al., 2010). Given previous observations of summer speed-up (Iken and Bindschadler, 1986; Zwally et al., 2002; Sundal et al., 2011; MacGregor et al., 2005; Bartholomaus et al., 2008),

TCD
8, 2611–2635, 2014

we may expect substantial erosion and transport during the melt season (Hermann et al., 2011).

However, the dynamics of basal water are yet to be fully understood, because high rate velocity measurements are still lacking particularly in the middle to upstream of mountain glaciers. Although high glacial erosion rates have been estimated from the St. Elias Mountains near the border of Alaska, USA, and Yukon, Canada (Fig. 1) (Humphrey and Raymond, 1994; Hallet et al., 1996), the ice velocity distribution has only recently been mapped (Burgess et al., 2013), and their spatial-temporal evolution remains unconstrained, limiting our understanding of the link between erosion processes and glacial hydrology. Moreover, numerous glaciers in the St. Elias Mountains are surge-type, which exhibit orders-of-magnitude speed-up during their active phase and are accompanied by km-scale terminus advance. While the Hubbard, Lowell, Tweedsmuir, and Chitina Glaciers indeed underwent mini-surges or surging during the period analyzed (Figs. 1–9), the mechanisms of glacier surge are still uncertain (Raymond, 1987; Harrison and Post, 2003). Understanding the mechanisms of glacier surge is also important to better simulate future ice dynamics, because significant contributions of the Alaskan glaciers' retreat to the possible sea level rise are predicted (Radic and Hock, 2011).

2 Data and analysis

We processed Phased Array-type L-band (wavelength of 23.6 cm) Synthetic Aperture Radar (PALSAR) images from the Advanced Land Observation Satellite (ALOS) operated by the Japan Aerospace Exploration Agency (JAXA), acquired along multiple paths (Fig. 1, Table 1). The pixel-offset tracking (or feature or speckle tracking) algorithms used in this study are based on maximising the cross-correlation of intensity image patches, which is essentially the same method used in previous studies (Strozzi et al., 2002; Yasuda and Furuya, 2013). We employed a search patch of 64 × 192 pixels (range × azimuth, ∼ 500 m × 500 m on the ground) and a sampling interval of 4 × 12 pixels (∼ 18 m × 18 m on the ground). The size of the search patch for the Hubbard Glacier was an exception; it was set at 128 × 384 pixels (range × azimuth, ∼ 1 km × 1 km on the ground) because of the larger size of the glacier. We set 4.0 as the threshold of the signal-to-noise ratio and patches below this level were treated as missing data. The FBD (fine-beam dual-polarisation mode) data are oversampled in the range direction so that the range dimension is the same as that of the FBS (fine-beam single-polarisation mode) data.

In performing pixel-offset tracking, we corrected for a stereoscopic effect included as artefact offsets over rugged terrain (Strozzi et al., 2002). Because of the separation between satellite orbital paths, the effect of foreshortening also differs in the offsets. We thus reduced the artifact by applying an elevation-dependent correction, incorporating the Advanced Spaceborne Thermal Emission and Reflection Radiometer (ASTER) Global Digital Elevation Model (GDEM) version 2 data with 30 m resolution.

Using both range and azimuth offset data, we derived the surface velocity data (Fig. 1) by assuming no vertical displacements. The studied glaciers are gently sloped at approximately 1–2°, and thus, the vertical component is much smaller than the horizontal component. In addition, we derived the velocity map using a pair of images that were temporally separated by at most 138 days. The glaciers' thinning during this period should be negligibly small in comparison to the horizontal movement of the glaciers. We averaged the velocity data over the ∼ 350 m × 350 m area along the flow line and estimated the measurement error to be less than 0.1 m d^{-1} from the standard deviation at each area.

3 Results

We examined spatial-temporal changes in the flow velocity of the glaciers during the period from December 2006 to March 2011 (Fig. 1). The detail of the data is listed on Table 1. After illustrating surging episodes at the three glaciers, we demonstrate

TCD
8, 2611–2635, 2014

winter speed-up signals at the other surge-type glaciers that were not surging during the analysis period.

3.1 Surging glaciers

3.1.1 Lowell Glacier

The latest surge of the Lowell Glacier began in the late 2009 and continued until around late 2010 (Yukon Geological Survey, 2011). While the ice velocity was at most $\sim 1\,\mathrm{m\,d^{-1}}$ from 2007 to 2009, it exceeded $5\,\mathrm{m\,d^{-1}}$ in the data pair of January and March 2010 (Fig. 2), which is consistent with the YGS report. The ice velocity slowed down in July and September 2010 (Fig. 2), but it is uncertain when it exactly terminated due to the lack of data.

Figure 3a indicates the terminus advance by as much as 4 km from early 2009 to July 2010. Figure 3b and c illustrates the radar intensity changes derived by the RGB method (Yasuda and Furuya, 2013). Radar intensity increases after the initiation of surging (Fig. 3b), whereas it decreases after the termination (Fig. 3c). We interpret that the intensity changes reflect the changes in the roughness of ice surface that are attributable to the opening and closure of crevasses by the surging.

3.1.2 Tweedsmuir Glacier

The United States Geological Survey (USGS) has been monitoring the Tweedsmuir Glacier. The largest surge occured around 2007 summer, and terminated in 2008 (The United States Geological Survey, 2010).

Figure 4 shows the ice velocity evolution, which exhibited a greater velocity with $\sim 6\,\mathrm{m\,d^{-1}}$ during the period from August to October 2007 but slowed down in January to March 2009. Figures 5a illustrates the terminus location changes, which expanded several hundreds of meters from the summer in 2007 to 2009. Figure 5b and c indicate the radar intensity changes associated with the surging episode.

3.1.3 A tributary of the Chitina Glacier

The Chitina glacier is one of the major surge-type glaciers composed of the Chitina River vally system. While the former surging episodes have been inferred from satellite image analyses (Clarke and Holdsworth, 2002), no ground-based monitoring has been performed at this glacier, to our knowledge.

Figure 6 illustrates the ice flow velocity time series at the Chitina Glacier. We notice that the velocity at the confluence in the lower reach increased in the fall 2009. At the same time, the radar scattering intensity also increased (Fig. 7a). We consider that the tributary in the lower reach underwent a surging episode that terminated around the summer 2010 in view of the flow velocity changes.

Figure 7 illustrates the radar intensity changes during (Fig. 7a) and after (Fig. 7b) the surging at the tributary. The intensity changes are probably associated with the surface roughness changes due to the opening and closure of crevasses.

3.2 Winter speed-up glaciers

We observed the winter speed-up signals at the seven glaciers (Chitina, Anderson, Walsh, Logan, Hubbard, Agassiz, and Donjek). The Anderson, Walsh, and Logan Glaciers (Fig. 1), which are also the major surge-type glaciers of the Chitina River valley system (Clarke and Holdsworth, 2002), could be examined with the highest temporal resolution because of the overlap of multiple satellite tracks (Fig. 1).

Figure 8 shows the spatial-temporal evolution of ice velocity at four glaciers along the flow lines illustrated in Fig. 1. At the Chitina Glaciers, the winter velocities in the upstream region of the glacier, exceeding $0.5\,\mathrm{m\,d^{-1}}$, were significantly greater than the fall velocities of $\sim 0.3\,\mathrm{m\,d^{-1}}$, regardless of the surge signal (Figs. 6 and 8a). At the 20 km point of the Anderson Glacier (Fig. 8b), the winter speed was more than double the fall speed. Along the upstream segment of the Walsh Glacier (Fig. 8c), the winter speed was more than 50 % greater than the fall speed. Moreover, in contrast to the upglacier propagation of summer speed-up (Zwally et al., 2002; Sundal et al., 2011; MacGregor

Discussion Paper | Discussion Paper | Discussion Paper | Discussion Paper |

TCD
8, 2611–2635, 2014

Winter speed-up of quiescent surge-type glaciers in Yukon, Canada

T. Abe and M. Furuya

et al., 2005), the higher-velocity region was observed to expand from upstream in fall to downstream in winter. This downglacier propagation was most clearly observed at the Anderson Glacier (Fig. 8b). While the flowline length and width of the Logan Glacier are nearly double those of the above three glaciers, the broad segment in the middle reach was also observed to accelerate from fall to winter (Fig. 8d). In addition, the winter velocities seemed to increase from one year to the next, indicating the initiation of the latest surging episode (Fig. 8d).

Although we could not obtain quality summer velocity data for each year (Burgess et al., 2013), the glacier dynamics at lower reaches seems to be normal. We observed clear summer speed-up signals in 2010 in the lower to middle reaches of each glacier (Fig. 8). However, the summer velocities in the upstream region of each glacier were comparable to the winter velocities, and the summer velocity was even slower than the winter velocity at the upstream region of the Walsh Glacier (Fig. 8c). In addition, the summer speed-up in the lower reaches appeared to occur primarily over a shorter period (Fig. 8). Furthermore, the lower reaches in winter exhibited the slowest velocities at all of the glaciers.

Hubbard Glacier is the longest and the only tidewater glacier in the study area (Fig. 1). Comparing the velocity at the measurement ~ 15 km section in the upstream region during the last summer (August to October) with that during the winter (January and February), the winter velocities (Fig. 9a, d, e, and h) were found to be 33–60 % greater than the late summer velocities. The significant speed-up during the 2009 winter was most likely associated with a small surge in the upper tributary (Fig. 9e). A tributary in the upper reach of the Malaspina Glacier (Fig. 1) also exhibited greater velocities in winter (Fig. 9a, d, e, and h), suggesting that the winter speed-up mechanism is independent of a given glacier's size. With the available data, we also confirmed the winter speed-up at the Donjek and Agassiz Glacier (Figs. 1, 10 and 11).

We also observed the winter speed-up signals at the Agassiz (Fig. 10) and the Donjek Glacier (Fig. 11). It should be noted that not all the glaciers could be examined as those in the Chitina River valley system with high temporal resolution. Increasing the

TCD
8, 2611–2635, 2014

data coverage in both space and time, it is likely that there are more winter speed-up glaciers. At Agassiz Glacier, the winter speed-up and downglacier propagation are confirmed from fall to winter in the 2007–2008, 2009–2010, and 2010–2011 seasons (Fig. 10); the winter velocities in 2008 and 2011 are obviously greater than the fall velocities in the corresponding years. We consider the greater velocity in the summer 2010 as the summer speed-up. Black-squared segment indicates the region of large seasonal fluctuations. At Donjek Glacier, comparing the velocities in the black-squared segment, we observe that the winter velocities are greater than the fall velocities (Fig. 11). However, the downglacier propagation is not clear.

4 Discussion

Surface meltwater depletion from fall to winter suggests that the mechanisms of the winter speed-up and its downglacier propagation are different from those of the summer speed-up that usually propagates upglacier. The detected annual winter speed-up is as much as 100 % too high to be explained by snow accumulation upstream. Given the ice thickness of ~ 550 m and an annual accumulation rate of ~ 1.5 m of water-equivalent at the 3017 m elevation of the Donjek Glacier (Clarke and Holdsworth, 2002) (Fig. 1), the annual equivalent ice thickness changes are at most ~ 0.3 %. Therefore, the speed-up caused by snow accumulation are expected less than ~ 1 %. Recalling that glacier surges in Yukon and Alaska are known to often begin in winter (Raymond, 1987; Harrison and Post, 2003), the observed winter speed-up in the upstream region may be regarded as a “mini-surge” (Humphrey and Raymond, 1994).

Based on a mechanism similar to that proposed for the 1982–1983 surge of the Variegated Glacier (Kamb et al., 1985) (Fig. 1), the efficient tunnel-shaped drainage system present in summer may provide a less efficient distributed system in winter because of the depletion of surface meltwater and the destruction of conduits by creep closure, and thus, the subglacial water pressure may be greatly increased. However, downglacier propagation of the winter speed-up will require such an efficient drainage system in the upstream that is usually found in the downstream closer to the terminus (Raymond et al., 1995). We need to consider any mechanisms that can trap water in the upstream in winter.

Using the few ERS1/2 tandem radar interferometry data with the 1–3 day's observation interval, Lingle and Fatland detected faster speed in winter than in fall at non-surging Seward Glaciers in the St. Elias Mountains (Lingle and Fatland, 2003). Moreover, the detected bull's eye-like localized signals at both surging and non-surging glaciers were interpreted to represent vertical motions of the surface caused by subglacial hydraulic phenomena. Given these observations combined with earlier glacier hydrological studies, they proposed englacial water storage and gravity-driven water flow toward the bed in winter regardless of whether a given glacier is surge-type or not (Lingle and Fatland, 2003).

We consider that our velocity measuments are complementary to the limited observations and revitalize the englacial water storage hypothesis. Each of the vertical glacier surface motions in the Lingle and Fatland's observation must be a transient short-term process that does not persist over a month or more, and that such vertical motions will be episodically occurring in places, because we did not observe any localized signals in our offset-tracking displacements that indicated greater horizontal displacements. However, presumably because rapid basal water pressure changes are accompanied with such vertical motions and also responsible for significant horizontal acceleration, it is likely that the cumulative horizontal displacements over a month and more are much greater than the vertical displacements.

Schoof et al. (2013) recently showed the records of wintertime water pressure oscillations at a surge-type glacier in Yukon, and interpreted them as spontaneous oscillations driven by water input not from the surface but from englacial sources or ground water flow. Due to the lack of flow velocity data, however, it was uncertain if the wintertime drainage phonemenon has any effects on the dynamics of glacier. The present observations of upstream winter speed-up also strongly support the presence of such water sources not directly connected to the glacier surface.

Although the presence of englacial water strorage can certainly account for the phase lag of the basal water flow behind the meltwater input (Fountain and Walder, 1998), neither the real picture nor the formation mechanisms of englacial water storage remain clear. However, one plausible form of englacial water storage is basal crevasse observed at Bench Glacier, Alaska (Harper et al., 2010). Because it has no direct route to the surface but can store significant volume of water near the bed, the water in the basal crevasses may generate high pressure when they become constricted due to creep closure in winter.

The formation of basal crevasses in grounded glaciers requires high basal water pressure that approaches ice overburden pressure and/or longitudinally extending ice flow (van deer Veen, 1998). These restricted conditions may explain the uncommon winter speed-up signals at the studied area. Taking the higher glacial erosion rates at the St. Elias Moutains into account, the longitudinal extension near the glacier bed in the middle to upstream region may be likely, because glacial erosion tends to develop an overdeepened concave bed topography (MacGregor et al., 2000; Anderson et al., 2006). The winter speed-up indeed starts from the upstream near-tributary areas of the Chitina, Walsh, and Anderson Glaciers (Figs. 1 and 8), where we may speculate the presence of such a concave basal topography. The basal water in the upstream accumulation zone, generated by infiltration of water in the firn layer and/or by basal ice melting caused by geothermal heat, could be trapped with high pressure under such basal topography.

5 Conclusions

In this paper, we show the spatial and temporal changes in the velocities near the border of Alaska and Yukon, applying offset tracking to the ALOS/PALSAR data from 2006–2011. We detected the ice flow velocity changes and the SAR intensity changes associated with the surging episodes at three glaciers (Lowell, Tweedsmuir and Chitina). Moreover, we revealed that upstream accelerations from fall to winter and its propagations to downstream at many quiescent surge-type glaciers around the St. Elias mountains. Combining the absence of upstream surface meltwater input in winter with the insights from some previous studies, we speculate that sizable water storages may be present near the bottom of glaciers without directly connecting to the surface, and that they could enhance basal sliding by increased water pressure as winter approaches. Although our velocity observations suggest the englacial water in the upstream, it remains unclear if such water storages are really present. Further observational and theoretical works are necessary to decipher the winter speed-up mechanisms.

Acknowledgements. The PALSAR level 1.0 data used in this study were provided by the PALSAR Interferometry Consortium to Study our Evolving Land surface (PIXEL) and the ALOS 3rd PI project, under cooperative research contracts with JAXA. The PALSAR data belong to JAXA and the Ministry of Economy, Trade, and Industry (METI). ASTER GDEM is a product of METI and NASA. We acknowledge KAKENHI (24651001) for supporting this study. We also thank S. Sugiyama and T. Sawagaki for discussion.

References

Anderson, R. S., Molnar, P., and Kessler, M. A.: Features of glacial valley profiles simply explained, J. Geophys. Res., 111, F01004, doi:10.1029/2005JF000344, 2006.

Bartholomaus, T. C., Anderson, R. S., and Anderson, S. P.: Response of glacial basal motion transient water storage, Nat. Geosci., 1, 33–37, 2008.

Berger, A. L., Gulick, S. P. S., Spotila, J. A., Upton, P., Jaeger, J. M., Chapman, J. B., Worthington, L. A., Pavlis, T. L., Ridgway, K. D., Willems, B. A., and McAleer, R. J.: Quaternary tectonic response to intensified glacial erosion in an orogenic wedge, Nat. Geosci., 1, 793–799, 2008.

Burgess, E. W., Foster, R. R., and Larson, C. F.: Flow velocities of Alaskan glaciers, Nat. Comms., 4, 2146, doi:10.1038/ncomms3146, doi:10.1038/ncomms3146, 2013.

Clarke, G. K. C. and Holdsworth, G.: Glaciers of the St. Elias Mountains, in: Satellite Image Atlas of Glaciers of the World, J301–J327, edited by: Williams Jr., R. S. and Ferrigno, J. G., USGS Professional Paper 1386-J, 2002.

Egholm, D. L., Nielsen, S. B., Pedersen, V. K., and Lesemann, J. E.: Glacial effects limiting mountain height, Nature, 460, 884–887, 2009.
Fountain, A. G. and Wald, J. S.: Water flow through temperate glaciers, Rev. Geophys., 36, 299–328, 1998.
Hallet, B.: Glacial quarrying: a simple theoretical model, Ann. Glaciol., 22, 1–8, 1996.
Hallet, B., Hunter, L., and Bogen, J.: Rates of erosion and sediment evacuation by glaciers: a review of field data and their implications, Global Planet. Change, 12, 213–235, 1996.
Harper, J. T., Bradford, J. H., Humphrey, N. F., and Meierbachtol, T. W.: Vertical extension of the subglacial drainage system into basal crevasses, Nature, 467, 579–582, 2010.
Harrison, W. D. and Post, A. S.: How much do we really know about glacier surging? An. Glaciol., 36, 1–6, 2003.
Hermann, F., Beaud, F., Campagnac, J. D., Lemieux, J. M., and Sternai, P.: Glacialhydrology and erosion patterns: a mechanism for carving glacial valleys, Earth Planet. Sc. Lett., 310, 498–508, 2011.
Humphrey, N. F. and Raymond, C. F.: Hydrology, erosion and sediment production in a surging glacier: variegated Glacier, Alaska, 1982–1983, J. Glaciol., 40, 539–552, 1994.
Iken, A. and Bindschadler, R. A.: Combined measurements of subglacial water pressures and surface velocity of the Findelengletscher, Switzerland. Conclusions about drainage systems and sliding mechanism. J. Glaciol., 32, 101–119, 1986.
Iverson, N. R.: Potential effects of subglacial water-pressure flucuations on quarrying, J. Glaciol. 37, 27–36, 1991.
Kamb, B., Raymond, C. F., Harrison, W. D., Engelhardt, H., Echelmeyer, K. A., Humphrey, N., Brugman, M. M., and Pfeffer, T.: Glacier surge mechanism: 1982–1983 surge of Variegated Glacier, Alaska, Science, 227, 469–477, 1985.
Lingle, C. S. and Fatland, D. R.: Does englacial water storage drive temperate glacier surge?, Ann. Glaciol. 36, 14–20, 2003.
MacGregor, K. R., Anderson, R. S., Anderson, S. P., and Waddington, E. D.: Numerical simulations of glacial-valley longitudinal profile evolution, Geology, 28, 1031–1034, 2000.
MacGregor, K. R., Riihimaki, C. A., and Anderson, R. S.: Spatial and temporal evolution of rapid basal sliding on Bench Glacier, Alaska, USA, J. Glaciol., 51, 49–63, 2005.
Radic, V. and Hock, R.: Regionally differentiated contribution of mountain glaciers and ice caps to future sea-level rise, Nat. Geosci., 4, 91–94, 2011.
Raymond, C. F.: How do glaciers surge? A review, J. Geophys. Res., 92, 9121–9134, 1987.

Raymond, C. F., Benedict, R. J., Harrison, W. D., Echelmeyer, K. A., and Strum, N.: Hydrological discharges and motion of fels and black rapid glaciers, Alaska, USA: implications for the structure of their drainage systems, J. Glaciol., 41, 290–304, 1995.

Schoof, C.: Ice-sheet acceleration driven by menlt supply variability, Nature, 468, 803–806, 2010.

Schoof, C., Rada, C. A., Wilson, N. J., Flowers, G. E., and Haseloff, M.: Oscillatory subglacial drainage in the absence of surface melt, The Cryosphere Discuss., 7, 5613–5657, doi:10.5194/tcd-7-5613-2013, 2013.

Strozzi, T., Luckman, A., Murray, T., Wegmuller, U., and Werner, C. L.: Glacier motion estimation using satellite-radar offset-tracking procedures, IEEE T. Geosci. Remote, 40, 2384–2391, 2002.

Sundal, A. V., Shepherd, A., Nienow, P., Hanna, E., Palmer, S., and Huybrechts, P.: Melt-induced speed-up of Greenland ice sheet offset by efficient subglacial drainage, Nature, 469, 521–524, 2011.

The United Nations Geological Survey: available at: http://ak.water.usgs.gov/Projects/Tweedsmuir/index.php (last access: 25 June 2013), 2010.

Thomson, S. N., Brandon, M. T., Tomkin, J. H., Reiners, P. W., Vásquez C., and Wilson, N. J.: Glaciation as a destructive and constructive control on mountain building, Nature, 467, 313–317, 2010.

van der Veen, C. J.: Fracture mechanics approach to penetration of bottom crevasses on glaciers, Cold Reg. Sci. Technol., 27, 213–223, 1998.

Yasuda, T. and Furuya, M.: Short-term glacier velocity changes at West Kunlun Shan, Northwest Tibet, detected by Synthetic Aperture Radar data, Remote Sens. Environ., 128, 86–106, 2013.

Yukon Geological Survey: available at: http://www.geology.gov.yk.ca/821.html (last access: 24 May 2013), 2011.

Zwally, H. J., Abdalati, W., Herring, T., Larson, T., Saba, J., and Steffen, K.: Surface melt-induced acceleration of greenland ice-sheet flow, Science, 297, 218–222, 2002.

TCD
8, 2611–2635, 2014

Table 1. Data list of the ALOS/PALSAR. The Bperp stands for the orbit separation distance perpendicular to the radar line of sight.

Sensor/Path	Frame	Master	Slave	Mode	Bperp (m)	Span (day)
PALSAR/241	1190–1210	20070829	20071014	FBD-FBD	597	46
		20080114	20080229	FBS-FBS	796	46
		20090116	20090303	FBS-FBS	529	46
		20100119	20100306	FBS-FBS	756	46
		20100306	20100421	FBS-FBS	353	46
		20100421	20100606	FBS-FBD	104	46
		20100606	20100722	FBD-FBD	122	46
		20100722	20100906	FBD-FBD	332	46
PALSAR/243	1200–1220	20061230	20070214	FBS-FBS	1342	46
		20070817	20071002	FBD-FBD	425	46
		20071002	20080102	FBD-FBS	627	92
		20080102	20080217	FBS-FBS	1041	46
		20080819	20090104	FBD-FBS	1779	138
		20090104	20090219	FBS-FBS	652	46
		20090822	20091007	FBD-FBD	566	46
		20091007	20100107	FBD-FBS	726	92
		20100107	20100222	FBS-FBS	794	46
		20100825	20101010	FBD-FBD	505	46
PALSAR/244	1200–1220	20070116	20070303	FBS-FBS	1554	46
		20070903	20071019	FBD-FBD	474	46
		20071019	20080119	FBD-FBS	799	92
		20080905	20081021	FBD-FBD	672	46
		20081021	20090121	FBD-FBS	874	92
		20090908	20091024	FBD-FBD	419	46
		20091024	20100124	FBD-FBS	960	92
		20100124	20100311	FBS-FBS	722	46
		20100911	20101027	FBD-FBD	504	46
PALSAR/244	1200–1220	20101027	20110127	FBD-FBS	997	92
		20110127	20110314	FBS-FBS	840	46
PALSAR/245	1200–1220	20070920	20071105	FBD-FBS	655	46
		20071105	20071221	FBS-FBS	86	46
		20071221	20080205	FBS-FBS	884	46
		20080807	20080922	FBD-FBD	1027	46
		20080922	20081223	FBD-FBS	596	92
		20090810	20090925	FBD-FBD	671	46
		20090925	20091226	FBD-FBS	776	92
		20091226	20100210	FBS-FBS	690	46
		20100210	20100328	FBS-FBS	532	46
		20100328	20100513	FBS-FBD	169	46
		20100513	20100628	FBD-FBD	122	46
		20100628	20100813	FBD-FBD	486	46
		20100813	20100928	FBD-FBD	470	46
		20100928	20101229	FBD-FBS	614	92
		20101229	20110213	FBS-FBS	790	46

TCD
8, 2611–2635, 2014

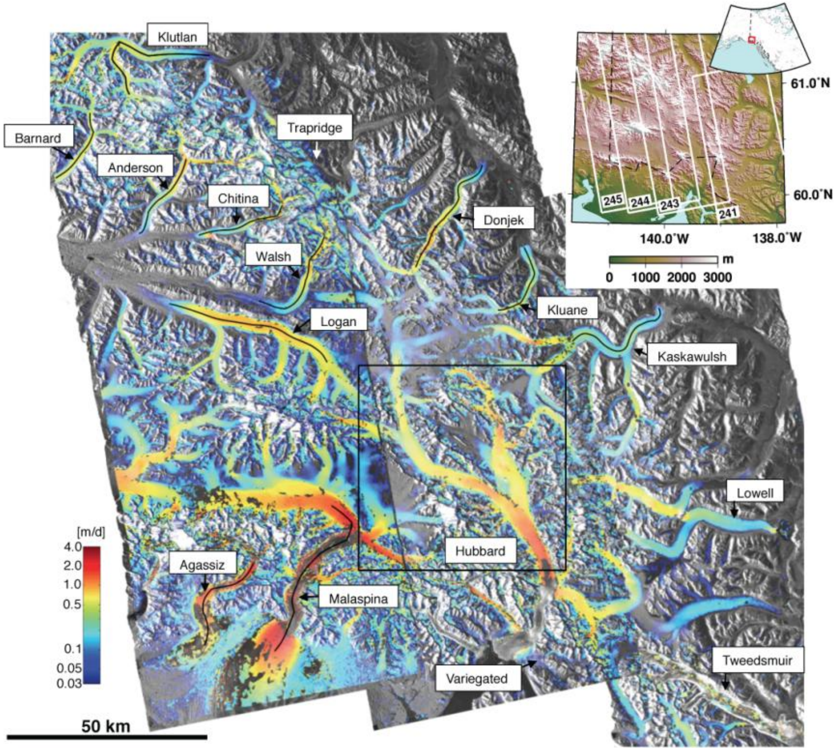

Figure 1. Ice velocity maps and location of the study area. Sample ice velocity maps for the study area derived by intensity tracking between two PALSAR images. The left, middle and right velocity maps are derived from images pairs from 10 February and 28 March 2010, 30 December 2006 and 14 February 2007, 14 January and 29 February 2008, respectively. The squared region of the Hubbard Glaciers is shown Fig. 9. The upper right panel indicates the location and topography of the study area as well as the satellite's imaging areas.

TCD
8, 2611–2635, 2014

Winter speed-up of quiescent surge-type glaciers in Yukon, Canada

T. Abe and M. Furuya

Title Page
Abstract | Introduction
Conclusions | References
Tables | Figures
◀| |▶
◀ ▶
Back | Close
Full Screen / Esc
Printer-friendly Version
Interactive Discussion

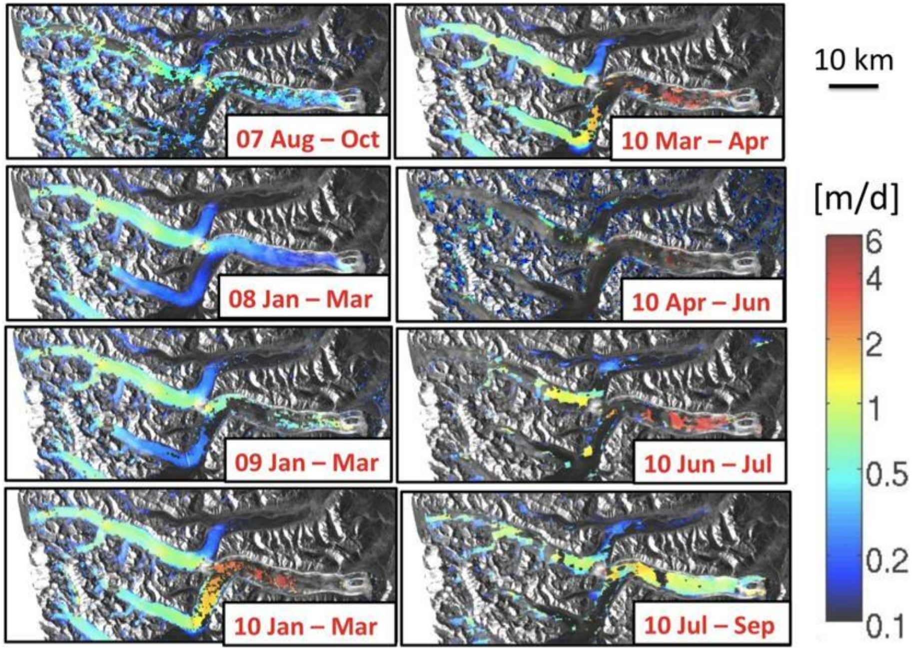

Figure 2. Surface velocity evolution at the Lowell Glacier. Please note the color scale is shown as logarithm.

TCD
8, 2611–2635, 2014

Winter speed-up of quiescent surge-type glaciers in Yukon, Canada

T. Abe and M. Furuya

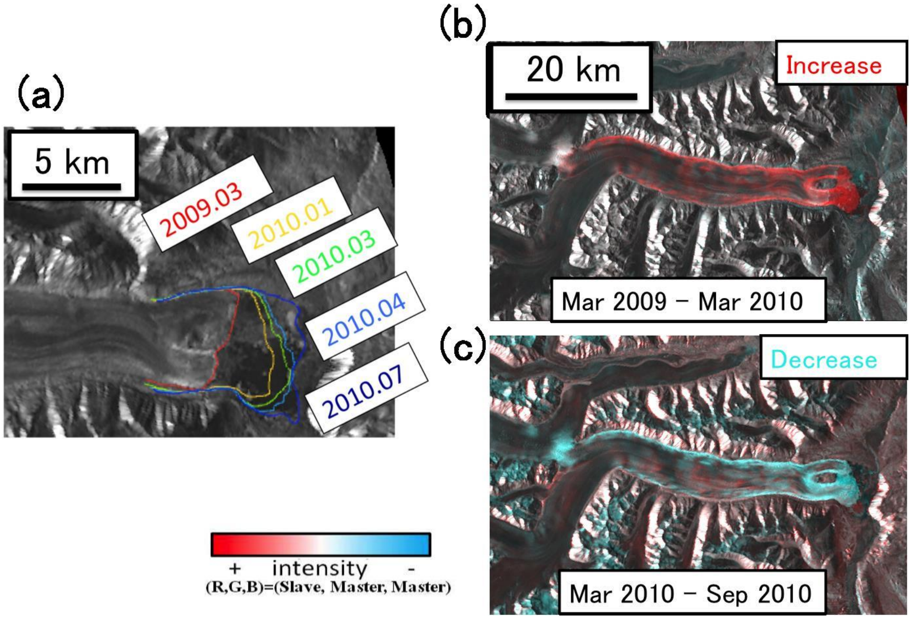

Figure 3. (a) Terminus advances at the Lowell Glacier recorded from PALSAR intensity images. **(b)** The RGB composite intensity image of an old image obtained on 3 March 2009 and a new image obtained on 6 March 2010. Red-colored area indicates an increase in the scattering intensity. **(c)** The composite image of an old image obtained on 3 March 2010 and a new image obtained on 10 September 2010. Cyan-colored area indicates a reduction in the scattering intensity.

TCD
8, 2611–2635, 2014

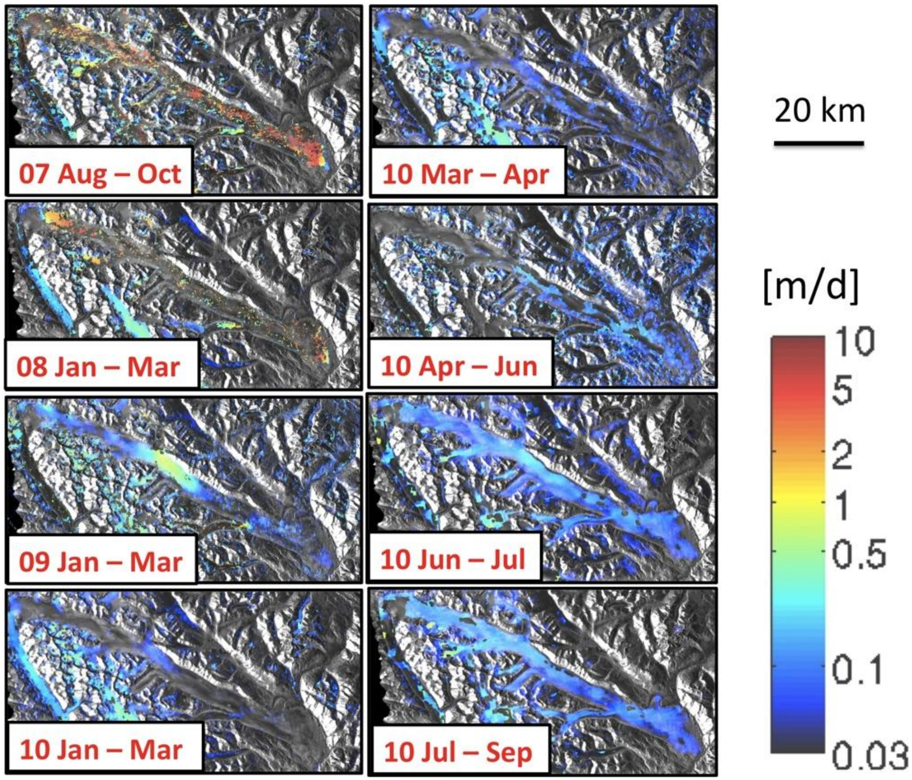

Figure 4. Surface velocity evolution at the Tweedsmuir Glacier. Please note the color scale is shown as logarithm.

TCD
8, 2611–2635, 2014

Winter speed-up of quiescent surge-type glaciers in Yukon, Canada

T. Abe and M. Furuya

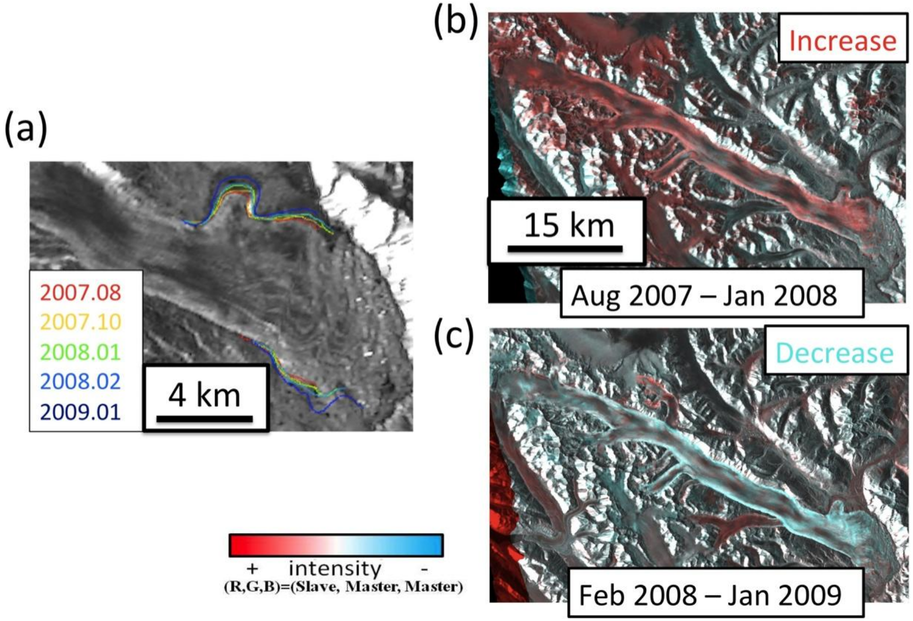

Figure 5. (a) Terminus advances at the Tweedsmuir Glacier. **(b)** The RGB composite intensity image of an old image obtained on 29 August 2007 and a new image obtained on 14 January 2008. **(c)** The composite image of an old image obtained on 29 February 2008 and a new image obtained on 16 January 2009.

TCD
8, 2611–2635, 2014

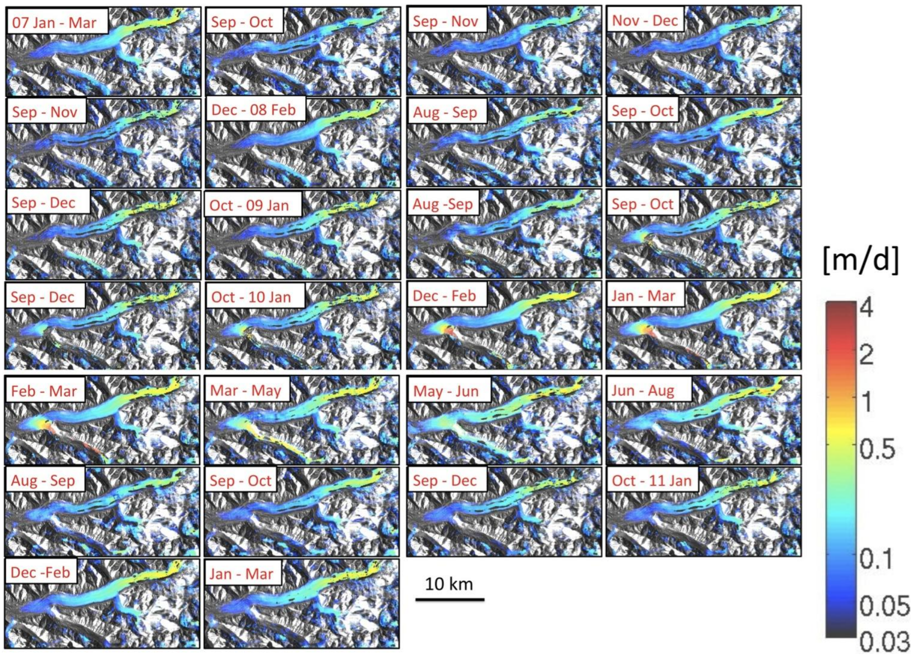

Figure 6. Surface velocity time-series (from upper left to lower right) at the Chitina Glacier. Please note the color scale is shown as logarithm. A surge occurred from autumn 2009 to summer 2010 at a tributary located in the lower reach.

TCD
8, 2611–2635, 2014

Winter speed-up of quiescent surge-type glaciers in Yukon, Canada

T. Abe and M. Furuya

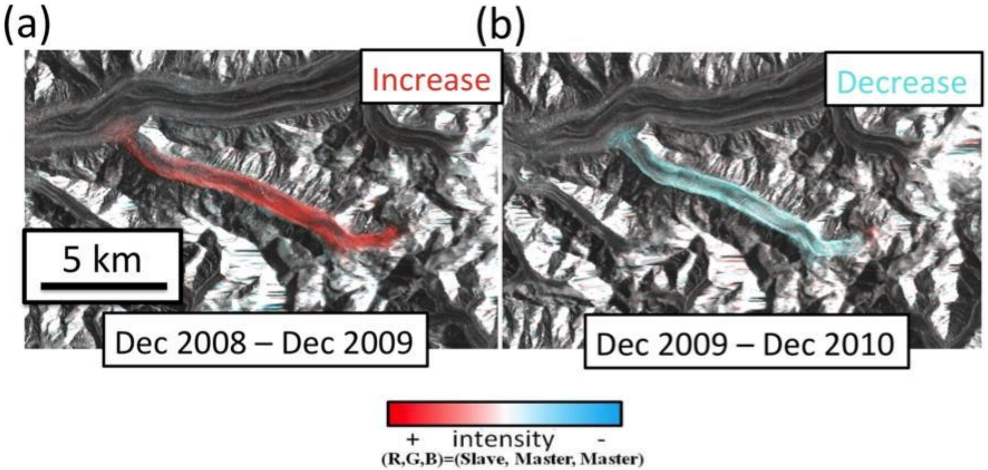

Figure 7. (a) The RGB composite intensity image of an old image obtained on 23 December 2008 and a new image obtained on 26 December 2009. **(b)** The composite image of an old image obtained on 26 December 2009 and a new image obtained on 29 December 2010.

TCD
8, 2611–2635, 2014

Winter speed-up of quiescent surge-type glaciers in Yukon, Canada

T. Abe and M. Furuya

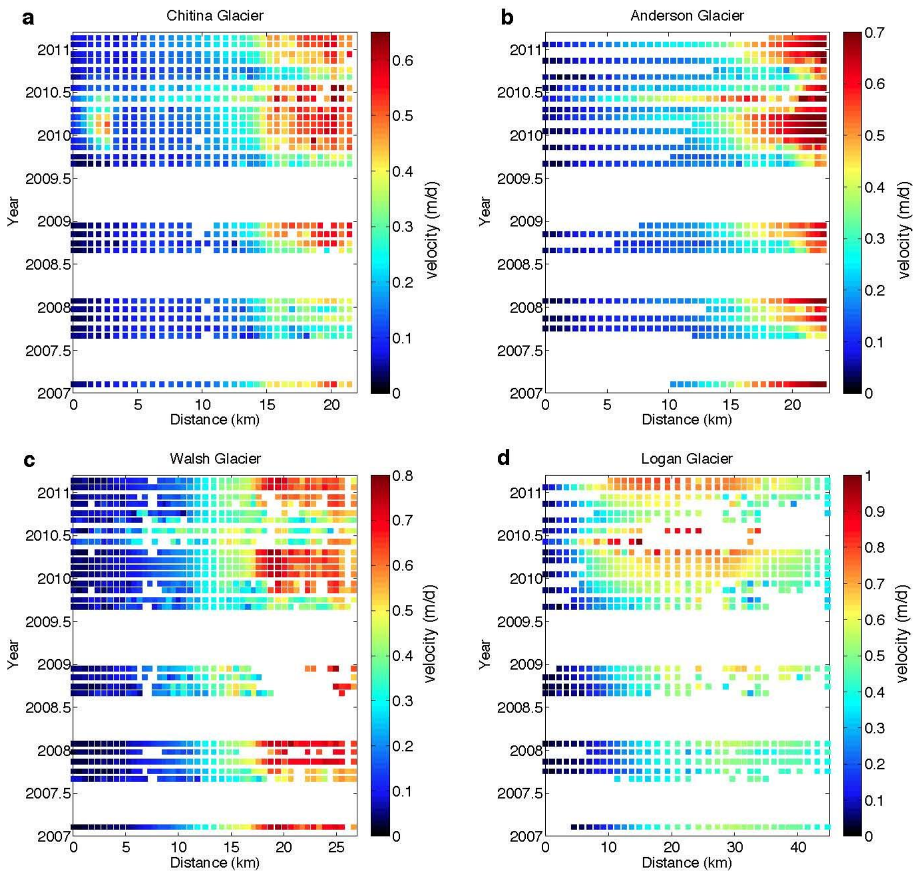

Figure 8. Spatial–temporal evolution of ice velocity at four glaciers in the study area. Ice velocity profiles along the flow line of the Chitina, Anderson, Walsh, and Logan Glaciers are shown as functions of time. The flow lines are illustrated in Fig. 1.

TCD
8, 2611–2635, 2014

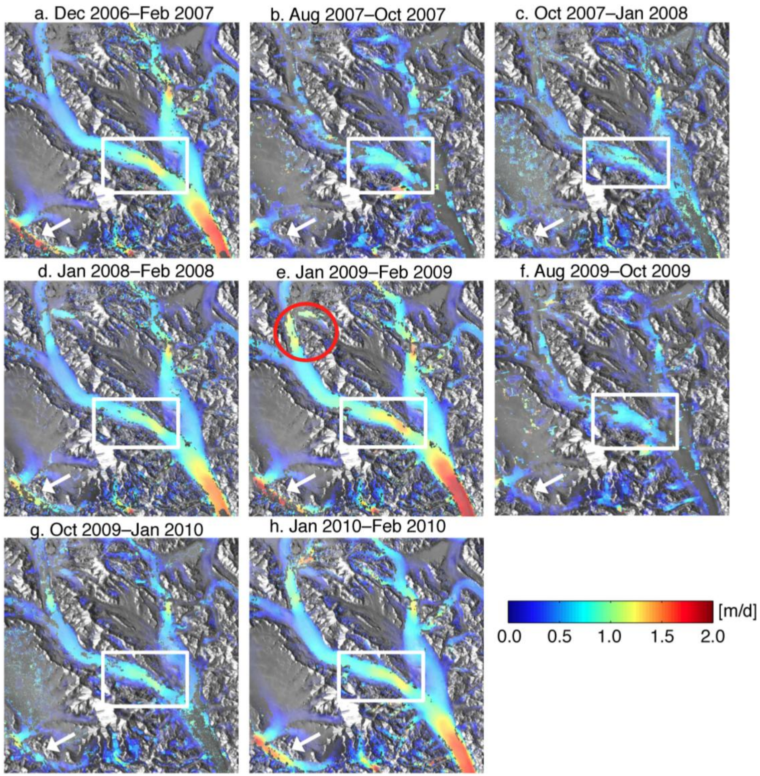

Figure 9. Spatial–temporal evolution of ice velocity at the Hubbard Glacier and an upper tributary of the Malaspina Glacier. The winter velocity at the measurable segment indicated by a white square **(a, d, e, h)** is greater than the velocity in late summer and fall **(b, c, f, g)**. We also observed a "mini-surge" signal **(e)** in the upstream region during January–February 2009. An upper tributary of the Malaspina Glacier, marked by a white arrow in the lower left, also exhibited winter speed-up.

TCD
8, 2611–2635, 2014

Winter speed-up of quiescent surge-type glaciers in Yukon, Canada

T. Abe and M. Furuya

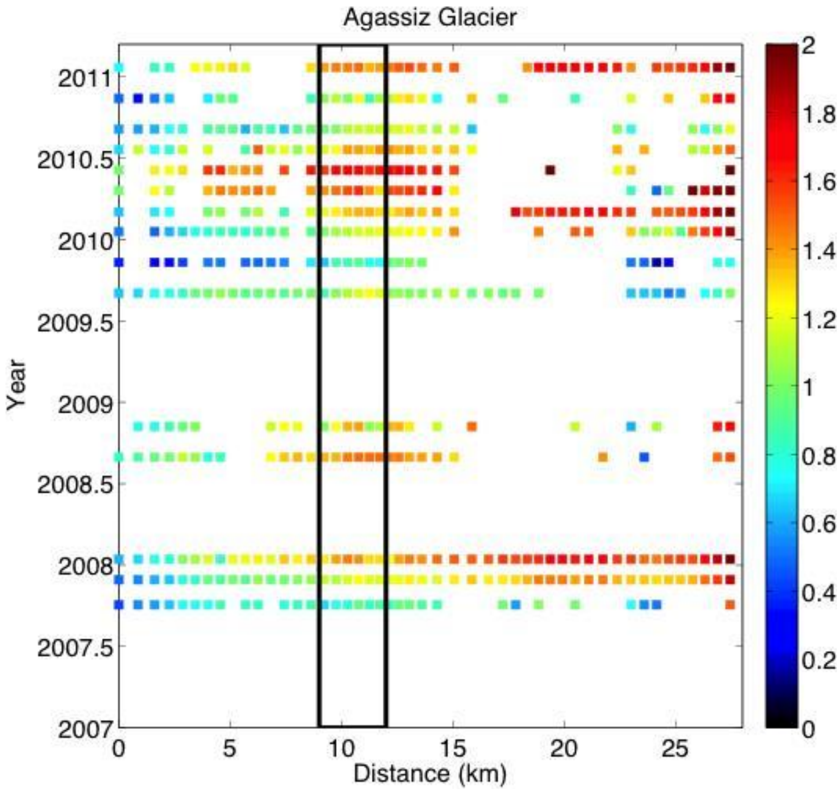

Figure 10. Spatial-temporal evolution of ice velocity at Agassiz Glacier from 2007 to 2011. The flow line indicated in Fig. 1.

TCD
8, 2611–2635, 2014

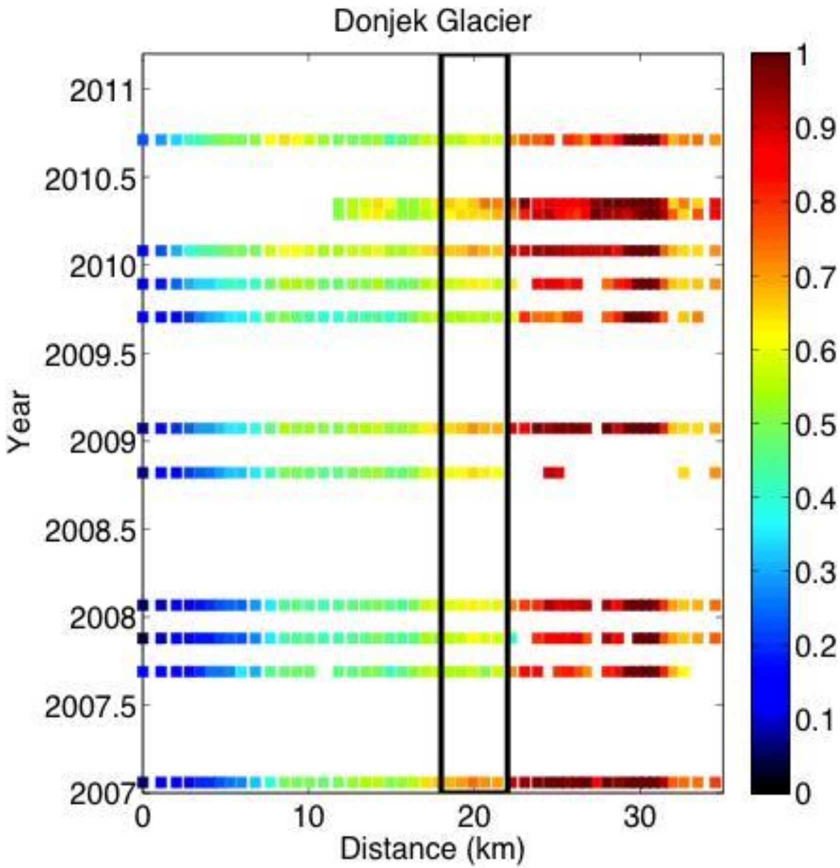

Figure 11. Spatial-temporal evolution of ice velocity at Donjek Glacier from 2007 to 2011. The flow line indicated in Fig. 1.

TCD
8, 2611–2635, 2014

Winter speed-up of quiescent surge-type glaciers in Yukon, Canada

T. Abe and M. Furuya

Title Page
Abstract Introduction
Conclusions References
Tables Figures
Back Close
Full Screen / Esc
Printer-friendly Version
Interactive Discussion